ELSEVIER

Polymer 41 (2000) 663–674

polymer

Synthesis and blends of pentabromobenzyl acrylate copolymers

G.D. Merfeld, T.T. Maa, K. Chan, D.R. Paul*

Department of Chemical Engineering and Texas Materials Institute, The University of Texas at Austin, Austin, TX 78712, USA

Received 4 August 1998; received in revised form 23 February 1999; accepted 24 February 1999

Abstract

The synthesis of styrene–pentabromobenzyl acrylate (S–PBBA) and methyl methacrylate–pentabromobenzyl acrylate (MMA–PBBA) copolymers and the phase behavior of their blends is reported. The miscibility of S–PBBA copolymers with polystyrene (PS), tetramethyl polycarbonate (TMPC), and poly(phenylene oxide) (PPO), and of MMA–PBBA copolymers with poly(methyl methacrylate) (PMMA) and polycarbonate (PC) was examined as a function of copolymer composition. Additionally, regions of miscibility were established for blends of both PBBA copolymer families with styrene–acrylonitrile (SAN) and styrene–maleic anhydride (SMA) copolymers, as well as for S–PBBA copolymers with styrene–methyl methacrylate (SMMA) copolymers. From the isothermal phase boundaries, repeat unit interaction energies with PBBA were estimated using previously established binary interaction energies, a binary interaction model, and the Flory–Huggins theory. In all cases, the interactions with PBBA were found to be highly endothermic. Lower critical solution temperature phase separation was measured for selected blends and compared with predictions based on the Sanchez–Lacombe equation-of-state. © 1999 Elsevier Science Ltd. All rights reserved.

Keywords: Copolymers; Blends; Miscibility

1. Introduction

Halogens can be incorporated into polymers to increase the glass transition temperature, improve thermal stability, alter permeability, tailor blend phase behavior, and impart flame retardancy [1,2]. Pentabromobenzyl acrylate (PBBA), see Fig. 1 for monomer structure, is of interest for these reasons. Its role as a flame retardant has been reported [3,4]; the incorporation of approximately 6–10 wt.% bromine in the form of a PBBA additive rendered various formulations of neat and glass-fiber reinforced nylon 6, nylon 6,6, PBT, and PET flame retardant to a UL-94 rating of V-0. Alternative to its use as an additive, introduction of the brominated species in a copolymer or in a miscible blend with the copolymer may have potential advantages related to processing, dispersion, and efficacy. In such blend systems, however, it is important to understand how phase behavior is affected by the presence of the brominated groups.

This paper describes the synthesis and characterization of PBBA copolymers with styrene and with methyl methacrylate, and reports the phase behavior of blends of these copolymers with other polymers. Both copolymer families were blended with their parent homopolymer, either polystyrene (PS) or poly(methyl methacrylate) (PMMA), to determine how much of the brominated monomer can be incorporated into a miscible blend and to quantify the interaction energy between the associated repeat units. Building upon this information, blends of the brominated copolymers with other homopolymers have been studied, specifically, blends of S–PBBA with tetramethyl polycarbonate (TMPC) and poly(phenylene oxide) (PPO), as well as blends of MMA–PBBA with polycarbonate (PC). Where applicable and of interest, blends with styrene–acrylonitrile (SAN), styrene–maleic anhydride (SMA), and styrene–methyl methacrylate (SMMA) copolymers are examined. Using a binary interaction model combined with the Flory–Huggins theory, interaction energies are calculated from phase behavior observations.

2. Polymer blend thermodynamics

The Gibbs free energy of mixing for a binary mixture of monodisperse polymers A and B is given by the Flory–Huggins theory [5,6]

$$\Delta g_{\text{mix}} = B\phi_A\phi_B + \mathrm{R}T\left[\frac{\rho_A\phi_A\ln\phi_A}{M_A} + \frac{\rho_B\phi_B\ln\phi_B}{M_B}\right] \quad (1)$$

where R is the gas constant, T is the absolute temperature, and ρ, ϕ, and M, are the density, volume fraction, and

---

* Corresponding author. Tel.: +1-512-471-5392; fax: +1-512-471-0542.
E-mail address: paul@che.utexas.edu (D.R. Paul)

PII: S0032-3861(99)00171-8

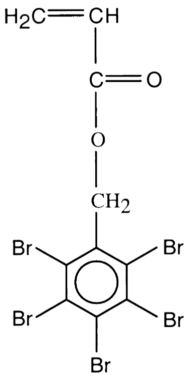

Fig. 1. Pentabromobenzyl acrylate monomer structure.

molecular weight, respectively. This free energy expression consists of contributions from combinatorial entropy, the bracketed terms, and an interaction energy B in which both the heat of mixing and other noncombinatorial effects are lumped. For equilibrium miscibility, Δg_{mix} should be negative and, for stability, its second derivative with respect to composition should be positive. Further, at the critical conditions of temperature and blend composition, where the third derivative with respect to composition is equal to zero and where the spinodal and binodal phase boundaries overlap, the balance between entropy and energetics is described by

$$B_{\mathrm{critical}} = \frac{\mathrm{R}T}{2}\left(\sqrt{\frac{\rho_{\mathrm{A}}}{(\bar{M}_{\mathrm{w}})_{\mathrm{A}}}} + \sqrt{\frac{\rho_{\mathrm{B}}}{(\bar{M}_{\mathrm{w}})_{\mathrm{B}}}}\right)^2. \tag{2}$$

For polydisperse polymers the weight average molecular weight, $\bar{M}_{\mathrm{w}}$, is properly used in this expression [7,8]. Isothermal miscibility is predicted when the net interaction energy B for a polymer mixture is more favorable than B_{critical}, i.e. $B < B_{\mathrm{critical}}$.

To describe the mixing energetics for a blend of a homopolymer and a copolymer or for a blend of two copolymers, a model must be invoked to treat the presence of both intra- and inter-molecular interactions. The binary interaction model accounts for such interactions and has been used with considerable success to interpret the phase behavior of blends involving copolymers [9–11]. The binary interaction model has the following forms

$$B = B_{12}\phi_2^2 \tag{3}$$

$$B = B_{12}\phi_2 + B_{13}\phi_3 - B_{23}\phi_2\phi_3 \tag{4}$$

$$B = B_{12}(\phi_2^2 - \phi_2\phi_3) + B_{13}(\phi_3^2 - \phi_2\phi_3) + B_{23}\phi_2\phi_3 \tag{5}$$

$$\begin{aligned} B = {} & B_{13}\phi_1\phi_3 + B_{14}\phi_1\phi_4 + B_{23}\phi_2\phi_3 + B_{24}\phi_2\phi_4 \\ & - B_{12}\phi_1\phi_2 - B_{34}\phi_3\phi_4 \end{aligned} \tag{6}$$

for blends of homopolymer 1 with copolymer 1–2, homopolymer 1 with copolymer 2–3, copolymer 1–2 with copolymer 1–3, and copolymer 1–2 with copolymer 3–4, corresponding to Eqs. (3)–(6), respectively. In these expressions, the volume fractions refer to the copolymer composition.

Table 1
PBBA copolymers

Copolymer	PBBA[a] (wt.%)	Molecular weight information[b]		T_g onset (°C)	Density (g/cm^3)	5% wt. loss temp. (°C)
		$\bar{M}_{\mathrm{w}}$	$\bar{M}_{\mathrm{n}}$			
S–PBBA10	19.8	95 800	61 600	108	–	372
S–PBBA20	33.9	113 400	67 800	110	–	365
S–PBBA30	44.9	65 800	41 400	115	–	375
S–PBBA40	54.0	34 900	19 800	117	–	377
S–PBBA50	60.3	47 200	24 500	124	–	374
S–PBBA60	66.3	38 000	18 300	127	–	374
S–PBBA70	72.6	64 200	41 800	134	–	372
S–PBBA80	74.1	66 600	45 100	139	–	364
MMA–PBBA10	8.2	106 000	75 000	110	1.241	293
MMA–PBBA20	15.8	92 000	62 000	118	1.331	283
MMA–PBBA30	23.7	92 000	64 000	123	1.391	287
MMA–PBBA40	31.9	85 000	56 000	120	1.463	295
MMA–PBBA50	39.8	87 000	58 000	124	1.533	313
MMA–PBBA60	47.4	85 000	59 000	127	1.640	317
MMA–PBBA70	58.4	87 000	47 000	125	–	320
MMA–PBBA80	70.9	89 000	54 000	134	–	327
MMA–PBBA90	80.5	62 000	37 000	146	–	332
PBBA100	100.0	–	–	178	2.54	342

[a] Determined by elemental analysis for bromine.
[b] Determined by GPC analysis using PS standards.

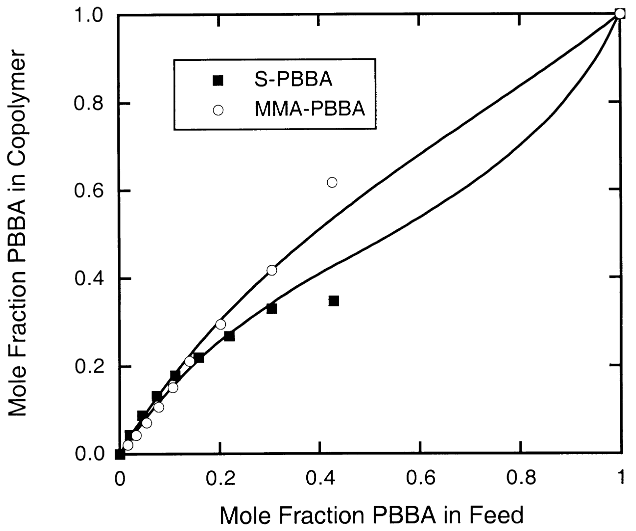

Fig. 2. Copolymer versus monomer feed composition for the free radical polymerization of PBBA with S and with MMA carried out to conversions of less than 15 wt.%. From the fits to the data shown, reactivity ratios given in the text were estimated.

3. Synthesis and characterization

Styrene and methyl methacrylate (both from Aldrich Chemical Co.) were copolymerized with pentabromobenzyl acrylate using AIBN as the free radical initiator. The copolymers produced in this study are listed in Table 1. The syntheses of S–PBBA copolymers and of the PBBA homopolymer have been reported previously [12]. Prior to reaction, inhibitors were extracted from the S and MMA monomers by washing twice with a 5% NaOH solution and then twice with distilled water. AIBN was purified by recrystallization from ethanol. The PBBA monomer, supplied courtesy of AmeriBrom Inc., was used as received with a melting point of 121.7°C. S–PBBA polymerizations were performed at 60°C in dioxane, except for the two lowest PBBA compositions which were carried out in bulk. MMA–PBBA polymerizations as well as the homopolymerization of PBBA were performed in toluene at 60°C. To preventing unzipping of the MMA, 5 wt.% of ethyl acrylate was added to the monomer feed of the two MMA–PBBA copolymers with the lowest PBBA contents. In order to minimize copolymer composition drift, reaction times were adjusted to keep conversions to less than 15%. All reactions were quenched in methanol and the recovered copolymer purified by repeated precipitation of a concentrated polymer/bromobenzene solution into hexane. After each reprecipitation, the copolymers were stirred in a large excess of hot methanol to extract any unreacted PBBA. Complete removal of PBBA monomer was confirmed by NMR. Copolymers were dried several days under vacuum and low heat before characterization.

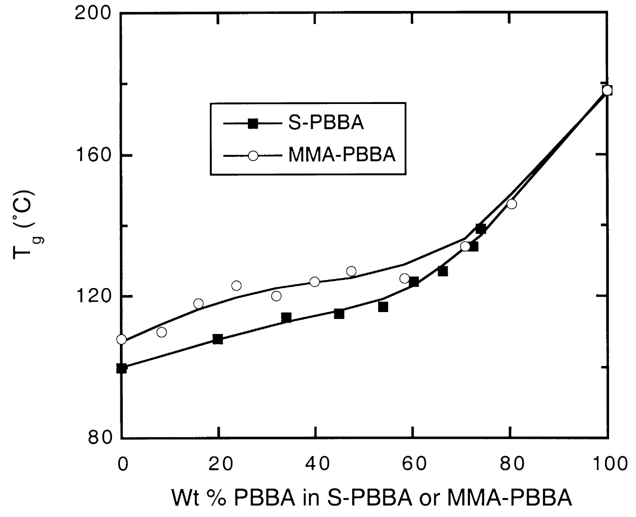

Fig. 3. Glass transition temperatures of S–PBBA and MMA–PBBA copolymers as a function of composition.

The numerical part of the acronym used to describe each copolymer in Table 1 corresponds to the wt.% PBBA charged to the reactor for synthesis. The actual PBBA incorporated into each copolymer was determined by elemental analysis for bromine by Atlantic Microlabs of Norcross, Georgia. A plot of monomer feed composition versus copolymer composition, in terms of PBBA mole fraction, is shown in Fig. 2. From the curve-fits shown, reactivity ratios were estimated for both copolymer families: for S–PBBA, $r_{\mathrm{PBBA}} = 0.4 \pm 0.1$ and $r_{\mathrm{S}} = 0.5 \pm 0.1$; for MMA–PBBA, $r_{\mathrm{PBBA}} = 0.9 \pm 0.2$ and $r_{\mathrm{MMA}} = 2.0 \pm 0.4$. It was difficult to accurately make copolymers with the higher mole fractions of PBBA because this required charging a very small amount of volatile S or MMA to the reactor. Since the lower composition measurements are believed to be more reliable, the curve-fits to the data were emphasized in this portion of the plot.

Other physical properties of the PBBA polymers are also summarized in Table 1. Molecular weights were evaluated by gel permeation chromatography (GPC) calibrated with polystyrene standards. Glass transition temperatures were measured by differential scanning calorimetry (DSC) with a Perkin–Elmer DSC-7 using a scan rate of 20°C/min; the values reported correspond to the onset condition. Fig. 3 shows that the glass transition temperatures of both copolymers are an increasing function of the PBBA content. For the PBBA homopolymer, a measured glass transition of 178°C is in good agreement with the previous report of 180°C [12]. Selected copolymer densities were measured in a density gradient column at 25°C using $CaNO_3$ solutions. An extrapolation of these values to 100% PBBA agrees well with the density of the PBBA homopolymer measured as 2.54 g/cm^3 in a solution of bromoform and carbon tetrachloride. The polymers were also tested by thermogravimetric analysis (TGA) in a Perkin–Elmer TGA-7 using a scan rate of 40°C/min. The temperatures at which the samples lost 5% of their total weight are reported. The thermal stability of the S–PBBA copolymers is largely invariant with composition while a slight increase with PBBA content

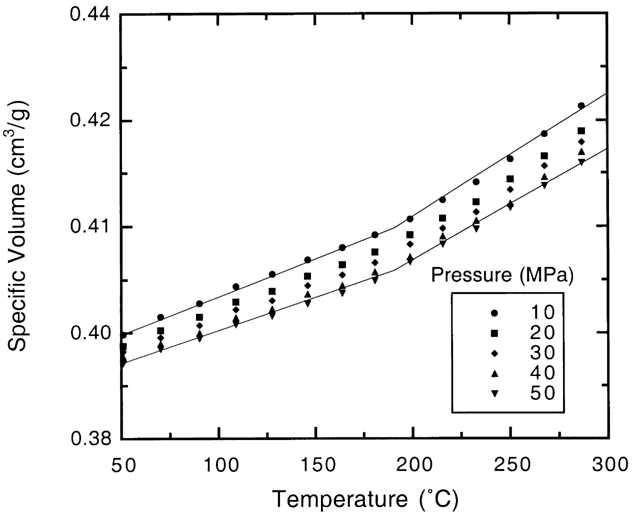

Fig. 4. PVT behavior of PBBA homopolymer measured in isothermal experiments. The intersection of isobaric lines corresponds to the glass transition temperature.

is recorded in the MMA–PBBA copolymers. Compared to a reference PMMA that contained approximately 5 wt.% ethyl acrylate to prevent depolymerization, all the MMA–PBBA copolymers studied here were more thermally stable.

Table 2
Homopolymers used in this study

Polymer[a]	Molecular weight information		T_g onset (°C)
	M_w	M_n	
PS	900 000	850 000	–
PS	330 000	100 000	105
PS	200 000	190 000	–
PS	100 000	94 000	–
PS	52 000	50 500	103
PS	30 300	29 400	–
PS	22 000	21 000	102
PS	17 500	16 300	101
PS	9200	8900	96
PS	4000	3800	–
PS	2000	1900	–
PS	800	700	–
PMMA	105 000	42 700	115
PMMA	60 000	56 000	126
PMMA	33 500	31 300	125
PMMA	20 300	18 300	125
PMMA	10 550	9500	108
PMMA	4250	4000	99
PMMA	2400	2200	77
PMMA	1400	1200	–
TMPC	37 900	13 700	190
PPO	39 000	29 400	218
PPO	32 000	17 900	–
PPO	23 900	15 500	–
PC	38 000	14 600	146
PC	29 900	10 800	142
PC	13 500	6200	138

[a] All materials obtained from commercial sources. The PS and PMMA are commercially available standards prepared by anionic polymerization.

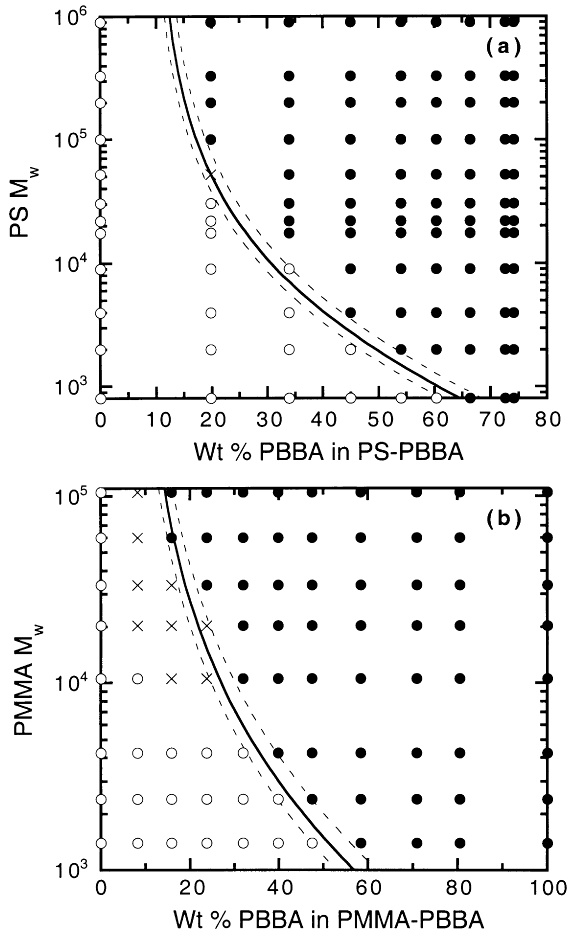

Fig. 5. Isothermal miscibility at 150°C for 50/50 blends of (a) PS of varying molecular weights with S–PBBA copolymers and of (b) PMMA of varying molecular weights with MMA–PBBA copolymers. Open circles indicate miscible blends while closed indicate immiscible blends. The curves shown were predicted using binary interaction energies of $B_{S/PBBA} = 4.0 \pm 0.7$ and $B_{MMA/PBBA} = 4.5 \pm 1.0$ cal/cm^3.

Finally, the equation-of-state properties of the PBBA homopolymer were measured in a Gnomix *PVT* apparatus. Fig. 4 shows representative *PVT* behavior obtained from experiments conducted isothermally. Isobaric lines are drawn to help identify the change in the slope of specific volume versus temperature at approximately 180°C which corresponds to the glass transition temperature.

4. Blend preparation and evaluation

Blends, 50/50 by weight, were prepared by casting from a common solvent, primarily bromobenzene, although THF was used in some limited cases as indicated. Solutions of the blends were hot cast on glass slides at 60°C. Films that were dry to the touch formed within 5 min, but were held at 60°C for an additional 15 min. Thereafter, the blends were annealed under vacuum at 150°C for 36 h or more. Visual assessments of blend miscibility were made both before and

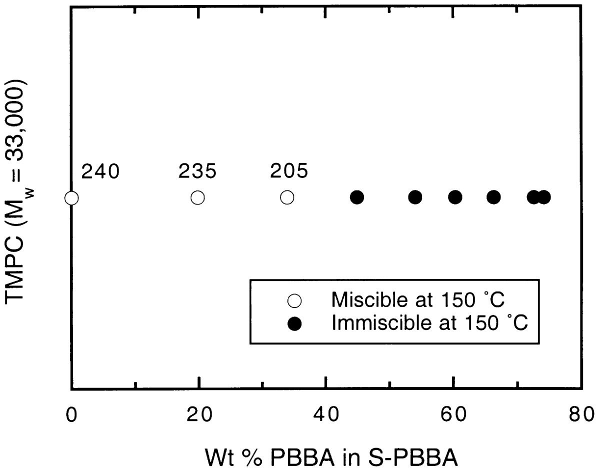

Fig. 6. Miscibility of 50/50 blends of TMPC with S–PBBA copolymers. LCST phase separation temperatures (°C) measured for the three miscible blends are indicated. The copolymer composition dependent miscibility was used to make an estimate of $B_{\mathrm{TMPC/PBBA}} = 3.4 \pm 0.7$ cal/cm^3.

after annealing. Phase behavior was also investigated by differential scanning calorimetry using a Perkin–Elmer DSC-7 at a scan rate of 20°C/min. Provided the component glass transitions were sufficiently different, a single transition located roughly midway between those of the components offered evidence of a miscible blend while two distinct glass transitions suggested an immiscible blend. Glass transition evaluations and visual assessments were used in combination.

Phase separation temperatures, all of the lower critical solution temperature (LCST) type, were bracketed below temperatures where a change from clear to cloudy or from one glass transition to two was recorded, and above temperatures where extended annealing times failed to induce phase separation [13]. When possible, rehomogenization was used to confirm reversibility of the phase separation process. Prohibitively slow rates of diffusion and thermal degradation, however, prevented verification of reversibility in some cases.

5. Blends of S–PBBA copolymers with PS

It is useful to know how much PBBA can be incorporated into S–PBBA and still maintain miscibility with PS. With this information, an independent assessment of the S/PBBA interaction energy can be made as well. Blends of the S–PBBA copolymers with polystyrenes (PS) of the varying molecular weights listed in Table 2 were made. The results at 150°C are summarized in Fig. 5(a) where open circles represent miscible blends and filled circles represent immiscible blends. As the single exception, a cross is used to indicate that the blend of PS ($\bar{M}_w = 52\,000$) with S–PBBA containing 19.8 wt.% PBBA could not be confidently defined as either miscible or immiscible. Overall, the miscibility distinction was sharp at lower PS molecular weights (<10 000) where both visual observation and DSC confirmed one another. It was more difficult to evaluate the state of miscibility in blends of higher molecular weight polystyrenes (>10 000) with copolymers containing small amounts of the brominated repeat unit (<25 wt.% PBBA) because, as the amount of PBBA decreases in the copolymer and the PS molecular weight increases, the physical properties of PS and S–PBBA become indistinguishable. For this reason, greater confidence is placed on the data that define the lower portion of the miscibility diagram.

A model predicting PS/S–PBBA phase behavior can be derived by combining Eqs. (2) and (3). Only one parameter, $B_{\mathrm{S/PBBA}}$, is unknown in the model and its value can be estimated by optimizing the fit to the data. A value of $B_{\mathrm{S/PBBA}} = 4.0$ cal/cm^3 was used to predict the solid curve separating miscible and immiscible blends in Fig. 5(a). The dashed curves on either side of the solid curve represent the largest acceptable deviation in the fit of the model, judged primarily on agreement with the lower portion of the diagram for the reasons discussed above. Accounting for this uncertainty in the fit of the model, a final estimate of $B_{\mathrm{S/PBBA}} = 4.0 \pm 0.7$ cal/cm^3 was obtained. These results indicate that polystyrene should be miscible with S–PBBA copolymers with PBBA contents of approximately 15 wt.% and less when both components have $\bar{M}_w = 100\,000$.

6. Blends of MMA–PBBA copolymers with PMMA

To investigate the miscibility limit of MMA–PBBA copolymers with PMMA and to quantify the MMA/PBBA interaction energy, MMA–PBBA copolymers were blended with the PMMA homopolymers listed in Table 2. The results from this study at 150°C are shown in Fig. 5(b). For certain blend compositions, the evaluation techniques were unable to determine the state of miscibility; crosses, rather than open (miscible) or filled (immiscible) circles, are used to denote these cases. They occur at the lowest PBBA compositions where the properties are most similar to the higher molecular weight PMMA homopolymers. The solid curve in Fig. 5(b) represents the best fit of a model derived by combining Eqs. (2) and (3). From it, an estimate of $B_{\mathrm{MMA/PBBA}} = 4.5$ cal/cm^3 was obtained. As in the PS/S–PBBA analysis, the quality of the model fit was emphasized in the lower half of the graph (for blends with PMMA molecular weights <10 000) because this is where confidence in the phase behavior observations is highest. By varying $B_{\mathrm{MMA/PBBA}}$ until the fit of the model approached the limits of acceptable agreement, represented by the dashed curves in Fig. 5(b), uncertainty in the binary interaction energy value was evaluated and incorporated in the estimate of $B_{\mathrm{MMA/PBBA}} = 4.5 \pm 1.0$ cal/cm^3. In general, the phase behavior is similar to that found in the PS/S–PBBA blend system but the tolerance for PBBA is slightly smaller as seen by comparing Fig. 5(a) and (b) and the interaction energies:

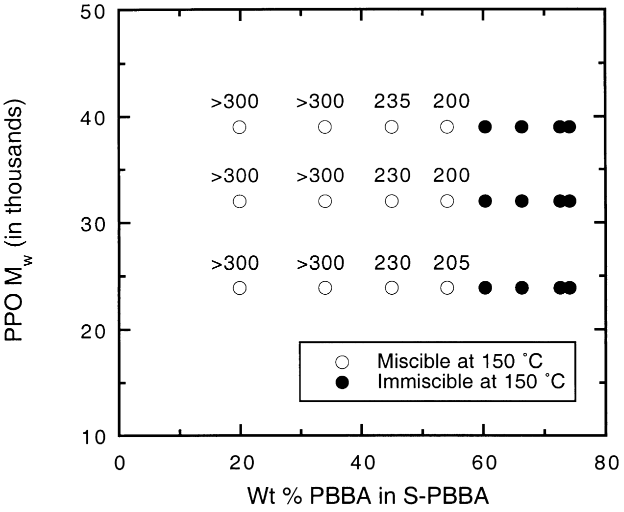

Fig. 7. PPO miscibility with S–PBBA copolymers (50/50 blends). Measured LCST phase separation temperatures (°C) are listed above the miscible blend compositions. Neither the miscibility boundary nor the phase separation temperature are affected by the change in PPO molecular weight. An estimate of $B_{PPO/PBBA} = 3.5 \pm 0.7$ was extracted from the phase behavior.

$B_{S/PBBA} = 4.0 \pm 0.7 < B_{MMA/PBBA} = 4.5 \pm 1.0$ cal/cm^3. Nevertheless, PMMA is expected to be miscible with MMA–PBBA copolymers containing approximately 15 wt.% or less PBBA, when both polymers have $\bar{M}_w = 100\,000$.

7. Blends of S–PBBA copolymers with TMPC

Blends of TMPC and PS, 50/50 by weight, are known to be miscible and to have a LCST of approximately 240°C. It is expected that some limited amount of PBBA may be incorporated into a copolymer with styrene and still maintain miscibility with TMPC. Determining how much PBBA can be tolerated provides information about the interaction energy between PBBA and TMPC. To investigate this, the TMPC homopolymer described in Table 2 was blended with the S–PBBA copolymers. The phase behavior of these blends at 150°C is summarized in Fig. 6. TMPC is miscible with the copolymers containing less than 33.9 wt.% PBBA and immiscible with the copolymers having more than 44.9 wt.% PBBA. The precise location of the boundary separating miscible and immiscible blends must lie between these copolymer compositions. Further, three binary interactions must be known to define the boundary, namely: $B_{TMPC/S}$, $B_{S/PBBA}$, and $B_{TMPC/PBBA}$. The TMPC/S interaction has been estimated elsewhere [14] to have a value of approximately -0.02 ± 0.01 cal/cm^3 and the S/PBBA interaction was evaluated earlier in this study to be 4.0 ± 0.7 cal/cm^3. An estimate for $B_{TMPC/PBBA}$ was made by fitting a model, derived by combining Eqs. (2) and (4), to the experimental phase behavior. Assuming the phase boundary lies at the PBBA 33.9 wt.% copolymer composition, an upper estimate of $B_{TMPC/PBBA} < 3.6 \pm 0.6$ cal/cm$_3$ is obtained. Similarly, if the phase boundary lies at the 44.9 wt.% PBBA copolymer composition, a lower estimate of $B_{TMPC/PBBA} > 3.2 \pm 0.6$ cal/cm^3 is obtained. Considering the uncertainty in the precise location of the phase boundary and in the previously known interaction energies, a final estimate of $B_{TMPC/PBBA} = 3.4 \pm 0.7$ cal/cm^3 is made.

The two TMPC/S–PBBA blends found to miscible at 150°C were tested for phase separation. The TMPC blend with S–PBBA containing 19.8 wt.% PBBA phase separated at 235 ± 5°C, and the blend with S–PBBA containing 33.9 wt.% PBBA phase separated at 205 ± 5°C. Since incorporating more PBBA into the copolymer increases the number of unfavorable interactions, it is not surprising that the phase separation temperature lowers accordingly.

8. Blends of S–PBBA copolymers with PPO

Blends of PPO and PS are completely miscible in all proportions and do not phase separate upon heating prior to thermal degradation. Therefore, blends of PPO with S–PBBA copolymers are expected to be miscible up to some limiting PBBA content. Since the PPO/S interaction is more favorable than the TMPC/S interaction, as is evidenced in part by the fact that PPO/PS blends do not phase separate whereas TMPC/PS blends phase separate at 240°C, PPO is expected to tolerate more PBBA in the S–PBBA copolymer. This was investigated by blending S–PBBA copolymers with the three PPO homopolymers listed in Table 2. The miscibility behavior measured at 150°C is summarized in Fig. 7. Irrespective of the PPO molecular weight, the phase boundary separating miscible from immiscible blends lies between S–PBBA copolymers containing 54.0 and 60.3 wt.% PBBA.

Two of the three interaction energies needed to define this phase boundary are known. Work earlier in this study produced an estimate of $B_{S/PBBA} = 4.0 \pm 0.7$ cal/cm^3 at 150°C while the several studies in the literature [10,15–17] suggest that the PPO/PS interaction falls within the range $B_{PPO/PS} = -0.42 \pm 0.1$ cal/cm^3 at 140°C. An upper and lower limit for $B_{PPO/PBBA}$ can be defined by assuming the phase boundary lies at copolymer compositions of 54.0 and 60.3 wt.% PBBA, respectively. A slight refinement to the interaction energy estimate is obtained by accounting for the various PPO molecular weights. The miscible blend of PPO $\bar{M}_w = 39\,000$ with S–PBBA containing 50.4 wt.% PBBA gives an upper limit of $B_{PPO/PBBA} < 3.8$ cal/cm^3, while the immiscible blend of PPO $\bar{M}_w = 23\,900$ with S–PBBA 60.3 wt.% PBBA provides a lower limit of $B_{PPO/PBBA} > 3.3$ cal/cm^3. A final estimate of $B_{PPO/PBBA} = 3.5 \pm 0.7$ cal/cm^3 is obtained after accounting for uncertainties in the previously known interaction energies.

Miscible PPO/S–PBBA blends were also investigated for phase separation behavior, and the LCST temperatures

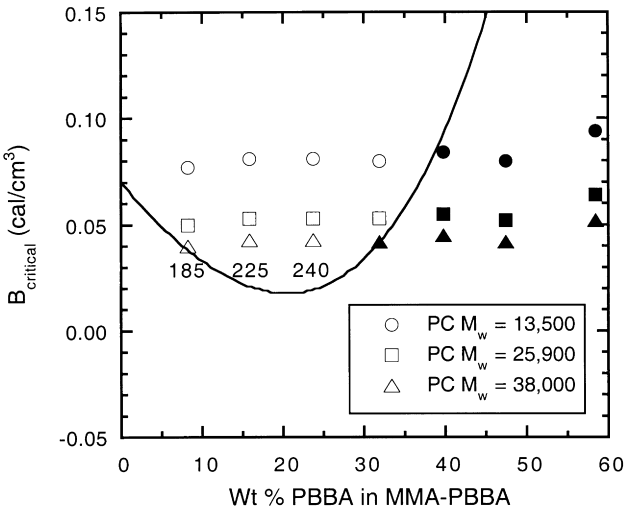

Fig. 8. Isothermal phase behavior for 50/50 blends of PC with MMA–PBBA copolymers at 150°C. The effect of molecular weight on miscibility, summarized in terms of $B_{critical}$ values calculated using Eq. (2), is considered as a function of copolymer composition. Open and closed symbols represent blends assessed to be miscible and immiscible, respectively, with the three PC molecular weights indicated. The best fit of the binary interaction model, given by Eq. (4), is shown as the solid line and is based on the following set of binary interaction energies: $B_{PC/MMA} = 0.07$, $B_{PC/PBBA} = 3.6$, and $B_{MMA/PBBA} = 4.5$ cal/cm^3.

included in Fig. 7 were measured. Like the miscible/immiscible phase boundary, PPO molecular weight had no real discernible effect on the observed phase separation temperatures. Conversely, phase separation temperatures appeared to be a strong function of copolymer composition: blends containing 33.9 wt.% PBBA and less did not phase separate at temperatures below 300°C, blends containing 44.9 wt.% PBBA phase separated at 230 ± 5°C, and blends with 54.0 wt.% PBBA phase separated at 200 ± 5°C. This trend is consistent with an increasingly unfavorable blend interaction as more PBBA is incorporated into the copolymer.

9. Blends of MMA–PBBA copolymers with PC

Commercial molecular weights of PC and PMMA are immiscible. It has been shown, however, that a copolymer of PMMA with a second, dissimilar monomer structure can be miscible with PC. This was investigated here for blends of the MMA–PBBA copolymers and the polycarbonates listed in Table 2. Similar blends have been disclosed in a patent application [18]. When the commercial grade PC ($\bar{M}_w = 38\,000$) was blended with the MMA–PBBA copolymers and annealed at 150°C, blends having 8.2, 15.8, and 23.7 wt.% PBBA were found to be miscible, and blends containing 31.9 wt.% PBBA and greater were all immiscible. These results prove that, indeed, miscibility with PC can be induced. From this information alone, however, it is difficult to extract a precise estimate for the PC/PBBA interaction energy.

Investigating how the region of miscibility broadens as PC molecular weight is lowered offers an opportunity to make a more refined estimate of $B_{PC/PBBA}$. To this end, polycarbonates having weight average molecular weights of 13 000 and 25 900 were also blended with the MMA–PBBA copolymers. The results of this study are summarized in Fig. 8. To enable consideration of both the PC and the copolymer molecular weights simultaneously, $B_{critical}$ was calculated for each blend using Eq. (2) and plotted versus the copolymer composition. The combinatorial entropy of mixing, and hence $B_{critical}$, increases as the PC molecular weight decreases. For blends with a given PC, the variability in the MMA–PBBA molecular weights reported in Table 1 is reflected in the $B_{critical}$ value. At the boundary separating miscible and immiscible blends, $B_{critical}$ must exactly balance the energetic contribution to mixing given by the binary interaction model in Eq. (4). Two of the three interaction energies needed to predict the phase boundary are known; $B_{PC/MMA}$ was calculated using results reported elsewhere [19] to be approximately 0.07 ± 0.01 cal/cm^3 at 150°C and $B_{MMA/PBBA}$ was estimated earlier in this work to have a value of 4.5 ± 1.0 cal/cm^3. An estimate for $B_{PC/PBBA}$ can be made by optimizing a fit of the model to the data. The solid line shown in Fig. 8 provides an estimate of $B_{PC/PBBA} = 3.6$ cal/cm$_3$. Uncertainty in this value was estimated by varying the known parameters within their confidence limits and adjusting $B_{PC/PBBA}$ until a good fit of the data was obtained. A reasonable fit of the data was always possible using interaction energies that fall within the range $B_{PC/PBBA} = 3.6 \pm 0.8$ cal/cm^3.

The three copolymers that were found miscible at 150°C with PC $\bar{M}_w = 38\,000$ had measured LCST phase separation temperatures of 185, 225, and 240°C, as indicated in the miscibility map. This trend does not follow the composition dependence for the PC/MMA/PBBA interaction curve shown in Fig. 8, perhaps suggesting that equation-of-state effects may be important. This will be investigated in a later discussion.

10. Blends of MMA–PBBA copolymers with styrenic copolymers

PMMA is known to be miscible with both SAN and SMA copolymers over a limited range of copolymer compositions. With SAN copolymers, the miscible range is from approximately 12–30 wt.% AN [20], and for SMA copolymers, the range is slightly larger, from approximately 10–35 wt.% MA [21]. Using these miscibility ranges with PMMA as a starting point, MMA–PBBA copolymers were blended with SAN and SMA copolymers; the physical properties of the latter are described in Table 3 where the numerical part of the copolymer acronym indicates the wt.% AN or MA. These materials have been described in more detail in previous studies [20–23]. In preparing these blends, it was necessary to use two different solvents owing to the fact that bromobenzene is not a good solvent for the styrenic copolymers containing the higher amounts

Table 3
Styrenic copolymers used in this study

Copolymer	Molecular weight information		T_g onset (°C)
	$\bar{M}_w$	$\bar{M}_n$	
Poly(styrene-co-acrylonitrile)			
SAN3.8	204 000	93 000	–
SAN5.5	212 000	–	106
SAN6.3	343 000	121 000	104
SAN10	195 600	94 700	104
SAN12.9	151 400	68 300	–
SAN15.2	197 000	–	105
SAN19.5	178 000	88 120	104
SAN25	152 000	77 000	107
SAN28.4	143 800	52 900	111
SAN30	160 000	81 000	109
SAN33	146 000	68 000	112
SAN40	122 000	61 000	113
Poly(styrene-co-maleic anhydride)			
SMA2	320 000	183 000	105
SMA4.7	179 000	94 000	106
SMA6	273 000	152 000	110
SMA8	200 000	100 000	115
SMA10.1	–	–	–
SMA14	178 000	92 000	125
SMA18.1	260 000	92 000	135
SMA25	252 000	69 700	149
SMA33	–	–	155
SMA47	–	–	147
SMA50	–	–	–
Poly(styrene-co-methyl methacrylate)			
SMMA4.5	281 000	98 000	98
SMMA9	96 000	44 000	98
SMMA10	106 000	59 100	–
SMMA13	164 000	67 000	98
SMMA15	106 000	60 000	–
SMMA20.5	270 000	12 000	98
SMMA25.5	150 000	57 000	–
SMMA32.5	167 000	78 000	95

of AN or MA, but THF is. Conversely, THF is a poor solvent for the MMA copolymers containing the higher amounts of PBBA whereas bromobenzene is a good solvent for these materials. Therefore, at high AN or MA contents, blends were prepared from THF, and at high PBBA contents bromobenzene was used.

The isothermal miscibility maps measured at 150°C are shown in Fig. 9(a) and (b) where the ordinate at 0 wt.% PBBA corresponds to blends of PMMA with SAN or SMA, respectively. In a limited number of situations, blends denoted with crosses could not be clearly distinguished as being either miscible or immiscible because the evaluation techniques were unable to distinguish the presence of two phases. However, for the two instances shown for blends with SMA, the close proximity to the miscibility boundary may have hindered interpretation. Despite these points, the region of miscibility with the SAN copolymers is well defined in Fig. 9(a). Slightly less well defined is the region of miscibility with the SMA copolymers in Fig. 9(b). Unfortunately, the unavailability of SMA copolymers containing between 35 and 45 wt.% MA leaves a small gap in the SMA miscibility map. In both the SAN and SMA miscibility maps, the homopolymer of PBBA and copolymers containing more than 60 wt.% PBBA are clearly immiscible. Similarly, the non-brominated version of the PBBA homopolymer, poly(benzyl acrylate), has been reported to be immiscible with SAN copolymers [24].

Since four different repeat unit types are present in each of these copolymer blends, six binary interaction energies are required to predict the regions of miscibility. Five of these are known for each map, some from previous studies and others from earlier in this work. Those interactions known from work elsewhere include $B_{S/AN} = 6.7–8.0$ [23,25–27]; $B_{S/MA} = 10.6–10.7$ [14,23]; $B_{S/MMA} = 0.18–0.26$ [23,28–30]; $B_{MMA/AN} = 4.1–4.5$ [26,30,31]; and a single report [23] gives $B_{MMA/MA} = 7.18\ \mathrm{cal/cm^3}$. For

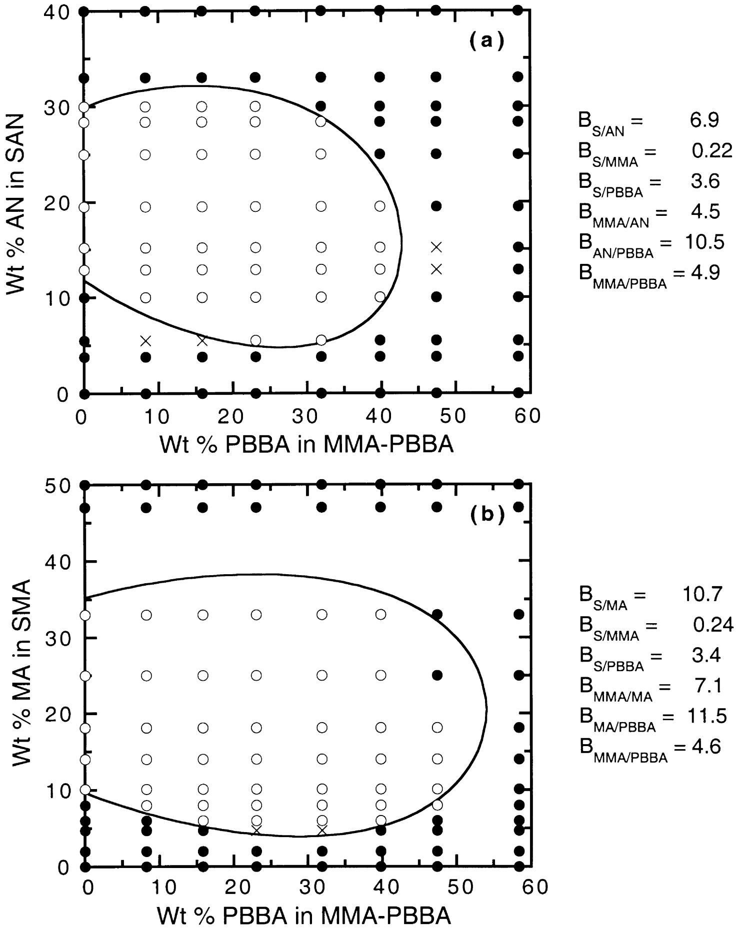

Fig. 9. Miscibility maps at 150°C for 50/50 blends of MMA–PBBA copolymers with (a) SAN copolymers and (b) SMA copolymers. The optimized fits of the binary interaction model shown produced estimates of $B_{\mathrm{AN/PBBA}} = 10.5 \pm 1.0$ and $B_{\mathrm{MA/PBBA}} = 11.5 \pm 1.5$ cal/cm^3.

conciseness, the ranges provided here are believed to encompass the most refined interaction energy estimates available. Values for the unknown interactions $B_{\mathrm{AN/PBBA}}$ and $B_{\mathrm{MA/PBBA}}$ can be extracted by fitting Eq. (6) to the experimental data. This procedure requires that the entropic contribution to mixing, described in terms of B_{critical}, is nearly the same for all blends within a given miscibility map. To a reasonable approximation this can be assumed here since the variation in component molecular weights is not too great. An average B_{critical} value representative of the blends that fall along the miscibility boundary is used in calculations.

The curves shown in Fig. 9 were identified by varying the known interactions within their confidence limits and adjusting the unknown parameters until a good fit was obtained. The best fit for the SAN map was found using a calculated average B_{critical} value of 0.02 cal/cm^3 and the set of parameters included in Fig. 9(a). Similarly, the best fit of the data for the SMA map was obtained using a calculated average B_{critical} value of 0.017 cal/cm^3 and the set of parameters included in Fig. 9(b). In general, the region of miscibility for blends with the SMA copolymers is larger than the region of miscibility with the SAN copolymers even though the AN/PBBA interaction is slightly more favorable than the MA/PBBA interaction. This is due, in part, to the significantly more endothermic interaction between S and MA in SMA compared to that for S and AN in SAN. The binary interaction model given by Eq. (6) reveals that the unfavorable intra-molecular interactions with AN, MA, and PBBA drive the miscibility in these blend systems.

Uncertainties in the unknown interactions were evaluated by varying all the established interactions within their known ranges and adjusting the value of the unknown parameter until a reasonable representation of the data was obtained. This procedure identified estimates of $B_{\mathrm{AN/PBBA}} = 10.5 \pm 1.0$ and $B_{\mathrm{MA/PBBA}} = 11.5 \pm 1.5$ cal/cm^3. The larger $B_{\mathrm{MA/PBBA}}$ uncertainty reflects, to some extent, the fact that the SMA miscibility map is less well defined than that for the SAN copolymers. Although the uncertainties assigned to both these interactions are larger than those determined for other interactions in this study, considering the magnitude of the interactions themselves, they represent a variability of only approximately ±10%.

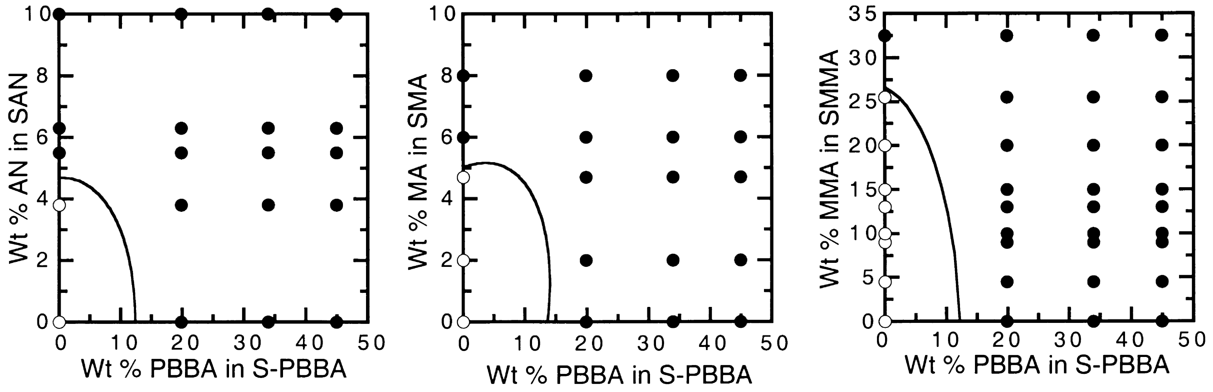

Fig. 10. Predicted and measured miscibility at 150°C for 50/50 blends of S–PBBA copolymers with SAN, SMA, and SMMA copolymers.

11. Blends of S–PBBA with styrenic copolymers

The opportunity to investigate blends of S–PBBA with SAN, SMA, and SMMA copolymers exists using the copolymers summarized in Table 3. Polystyrene ($\bar{M}_w = 100\,000$) has been shown to be miscible with SMMA copolymers ($\bar{M}_w = 100\,000$) containing less than about 25 wt.% MMA [23], and with SAN or SMA copolymers ($\bar{M}_w = 200\,000$) containing approximately 5 wt.% and less of either AN or MA [22,23]. All the interaction energies needed to predict the copolymer/copolymer regions of miscibility have now been determined here or elsewhere; those interactions needed from other studies have been introduced already in the preceding work. The results of these calculations at 150°C are shown in Fig. 10 as the solid curves. In each case only a small region of miscibility is predicted. In fact, is was not possible to formulate blends expected to be miscible using the copolymer compositions available. Even though the experimental observations included in Fig. 10 cannot help refine the estimated binary interactions, they are consistent nonetheless with the predictions.

12. Equation-of-state prediction of phase separation

LCST type phase separation temperatures were recorded in this work for blends with TMPC, PPO, and PC. The Flory–Huggins theory cannot predict this type of phase behavior without empirical modification because it assumes incompressibility of the polymer mixture. Alternatively, equation-of-state theories allow for compressibility effects and naturally predict LCST phase separation. Using the binary interaction energies evaluated earlier, an equation-of-state prediction of phase separation temperatures can be made and compared with experimental values. For this, the lattice fluid theory of Sanchez and Lacombe was used [32–34]. It is a corresponding states theory that uses measured characteristic *PVT* parameters and $\Delta P_{ij}{}^*$ interaction energies stripped free of compressibility effects unlike the Flory–Huggins B_{ij} interaction energies. The calculations involve converting each B_{ij} to a corresponding $\Delta P_{ij}{}^*$ and solving the Sanchez–Lacombe equation-of-state under the thermodynamic constraints of the spinodal condition. The details of these calculations have been explained elsewhere [14,35]. Experimental *PVT* measurements for the PBBA homopolymer were introduced in Fig. 4. From these data, characteristic Sanchez–Lacombe parameters were deduced and are listed in Table 4 along with other relevant parameters taken from the literature [13,19,23,30,36].

Phase separation temperatures previously reported in Figs. 6–8 are compiled in Table 5 to allow comparison with the predicted values. Blends that border the phase boundary but were immiscible at 150°C are included in the table; these are denoted with phase separation temperatures of <150°C. In all three blend systems, the location of the 150°C phase boundary is predicted correctly to fall between the appropriate blend compositions. And although the magnitude of the predictions does not match that of the

Table 4
Sanchez–Lacombe characteristic parameters

Repeat unit type	P^* (MPa)	T^* (K)	ρ^* (g/cm^3)	Temperature range (°C)	Reference
PBBA	516	940	2.610	200–270	This study
PS[a]	379	795	1.097	200–250	[23,36]
PMMA	509	742	1.256	220–270	[19]
TMPC	440	729	1.185	220–270	[13]
PPO	408	758	1.173	220–270	[30]
PC	496	802	1.276	210–270	[19]

[a] Recalculated from data in reference.

Table 5
Comparison of experimentally measured and predicted phase separation temperatures (°C)

Blend	Experiment	Sanchez–Lacombe
TMPC/PS	240	280
TMPC/S–PBBA10	235	280
TMPC/S–PBBA20	210	190
TMPC/S–PBBA30	< 150	85
PPO39K/PS	> 300	> 1000
PPO39K/S–PBBA10	> 300	995
PPO39K/S–PBBA20	> 300	775
PPO39K/S–PBBA30	235	575
PPO39K/S–PBBA40	200	325
PPO39K/S–PBBA50	< 150	< 100
PC38K/PMMA	< 150	20
PC38K/MMA–PBBA10	185	170
PC38K/MMA–PBBA20	225	320
PC38K/MMA–PBBA30	240	560
PC38K/MMA–PBBA40	< 150	< 100

measurements, the trends with changing copolymer composition follow those recorded experimentally. Specifically, it was noted earlier that the phase separation temperatures measured for PC ($\bar{M}_w = 38\,000$) with MMA–PBBA copolymers did not follow the trend of the Flory–Huggins interaction energy, but accounting for equation-of-state effects provides a good representation of the behavior. Prior work has shown that phase separation temperature predictions can be extremely sensitive to the parameters used in the theory, and so the agreement found here is significant [14,23].

13. Conclusions

The synthesis, characterization, and blend properties of S–PBBA and MMA–PBBA copolymers have been reported. The regions of copolymer composition that lead to isothermal miscibility of S–PBBA copolymers with PS, TMPC, and PPO homopolymers, and of MMA–PBBA copolymers with PMMA and PC were identified. Using the Flory–Huggins theory combined with a binary interaction model, the interaction energies of PBBA with PS, PMMA, TMPC, PPO, and PC were extracted from isothermal phase behavior. Additionally, by studying blends of MMA–PBBA copolymers with both SAN and SMA copolymers, the interaction energies of PBBA with AN and with MA were estimated. Predictions of S–PBBA miscibility with SAN, SMA, and SMMA copolymers based on these interactions energies were consistent with limited experimental observations. A summary of the interactions determined in this study is compiled in Table 6 and includes estimates of the confidence to which the parameters are known. In all cases, the interactions are highly endothermic. The PBBA interactions with TMPC, PPO, and PC are of equal value within the uncertainty limits, perhaps related to the phenolic structure common in their repeat units. The interactions with S and MMA are slightly less favorable, and the interactions with AN and MA are considerably less favorable. Phase separation temperatures predicted by equation-of-state theory agree with the isothermal miscibility limits and with trends observed in copolymer composition dependence, but not with the magnitude of the experimental values.

Table 6
Summary of binary interaction energies (cal/cm^3) determined in this study at 150°C

Binary pair	B_{ij} with confidence limits
S/PBBA	4.0 ± 0.7
MMA/PBBA	4.5 ± 1.0
TMPC/PBBA	3.4 ± 0.7
PPO/PBBA	3.5 ± 0.7
PC/PBBA	3.6 ± 0.8
AN/PBBA	10.5 ± 1.0
MA/PBBA	11.5 ± 1.5

Acknowledgements

Financial support for this work was provided by the National Science Foundation grant numbers DMR 92-15926 and DMR 97-26484 administered by the Division of Materials Research—Polymers Program.

References

[1] Fire FL. Combustibility of plastics. New York: van Nostrand Reinhold, 1991.
[2] Troitzsch J. Makromol Chem Macromol Symp 1993;74:125.
[3] Siegman A, Yanai S, Dagan A, Cohen Y, Rumack M, Georlette P. Poly (pentabromobenzyl acrylate), a novel flame-retardant additive for engineering thermoplastics. In: Price D, Iddon B, Wakefield BJ, editors. Proceedings of the International Conference on Chemical Applications of Bromine and its Compounds. Amsterdam: Elsevier, 1988. p. 339.
[4] Dave V, Israel SC. Am Chem Soc Polym Prepr 1990;31:554.
[5] Flory PJ. J Chem Phys 1942;10:51.
[6] Huggins ML. J Chem Phys 1941;9:440.
[7] Koningsveld R, Chermin HAG. Proc Royal Soc London A 1970;319:331.
[8] Koningsveld R, Kleintjens LA. J Polym Sci Polym Symp 1977;61:221.
[9] Kambour RP, Bendler JT, Bopp RC. Macromolecules 1983;16:753.
[10] ten Brinke G, Karasz FE, MacKnight WJ. Macromolecules 1983;16:1827.
[11] Paul DR, Barlow JW. Polymer 1984;25:487.
[12] Yuan Y, Siegmann A, Narkis M. J Appl Polym Sci 1996;60:1475.
[13] Kim CK, Paul DR. Polymer 1992;33:1630.
[14] Merfeld GD, Paul DR. Polymer 1998;39:1999.
[15] ten Brinke G, Rubinstein E, Karasz FE, MacKnight WJ, Vukovic R. J Appl Phys 1984;56:2440.
[16] Maconnachie A, Kambour RP, White DM, Rostami S, Walsh DJ. Macromolecules 1984;17:2645.

[17] Composto RJ, Mayer JW, Kramer EJ, White DM. Phys Rev Lett 1986;57:1312.

[18] Ohnaga T, Sato T, Nagata S, Ohtani M, Arakawa K, Hasegawa T. European Patent Application Patent No. 92152402, 1991, Kuraray Co. Ltd.

[19] Callaghan TA, Paul DR. J Polym Sci Part B: Polym Phys 1994;32:1813.

[20] Fowler ME, Barlow JW, Paul DR. Polymer 1987;28:1177.

[21] Brannock GR, Barlow JW, Paul DR. J Polym Sci Part B: Polym Phys 1991;29:413.

[22] Kim JH, Barlow JW, Paul DR. J Polym Sci Part B: Polym Phys 1989;27:223.

[23] Gan PP, Paul DR. J Appl Polym Sci 1994;54:317.

[24] Sankarapandian M, Kishore K. Macromolecules 1994;27:7278.

[25] Keitz JD, Barlow JW, Paul DR. J Appl Polym Sci 1984;29:3131.

[26] Nishimoto M, Keskkula H, Paul DR. Polymer 1989;30:1279.

[27] Nishimoto M, Keskkula H, Paul DR. Macromolecules 1990;23:3633.

[28] Fukuda T, Nagata M, Inagaki H. Macromolecules 1986;19:1411.

[29] Callaghan TA, Paul DR. Macromolecules 1993;26:2439.

[30] Gan PP, Padwa AR, Paul DR. Polymer 1994;35:1487.

[31] Chu J, Paul DR. Polymer 1999;40:2687.

[32] Sanchez IC, Lacombe RH. Macromolecules 1978;11:1145.

[33] Sanchez IC. Polymer phase separation. In: Meyers RA, editor. Encyclopedia of physical science and technology, vol. 13. New York: Academic Press, 1992.

[34] Sanchez IC, Panayiotou CG. Equation of state, thermodynamics of polymer and related solutions, ch. 3. In: Sandler SI, editor. Models of thermodynamic and phase equilibrium calculations. New York: Marcel Dekker, 1994.

[35] Callaghan TA. PhD Dissertation, The University of Texas at Austin, 1992.

[36] Gan PP. PhD Dissertation, The University of Texas at Austin, 1994.